Intracellular degradation of low-density lipoprotein probed with two-color fluorescence microscopy†

William H. Humphries IV, Nicole C. Fay and Christine K. Payne*

Received 17th May 2010, Accepted 3rd August 2010
DOI: 10.1039/c0ib00035c

The intracellular vesicle-mediated degradation of extracellular cargo is an essential cellular function. Using two-color single particle tracking fluorescence microscopy, we have probed the intracellular degradation of low-density lipoprotein (LDL) in living cells. To detect degradation, individual LDL particles were heavily labeled with multiple fluorophores resulting in a quenched fluorescent signal. The degradation of the LDL particle then resulted in an increase in fluorescence. Endocytic vesicles were fluorescently labeled with variants of GFP. We imaged the transient colocalization of LDL with endocytic vesicles while simultaneously measuring the intensity of the LDL particle as an indicator of degradation. These studies demonstrate that late endosomes are active sites of degradation for LDL. Measurement of the time from colocalization with lysosome-associated membrane protein 1 (LAMP1) vesicles to degradation suggests that LAMP1-vesicles initiate the degradative event. Observing degradation as it occurs in living cells makes it possible to describe the complete endocytic pathway of LDL from internalization to degradation. More generally, this research provides a model for the intracellular degradation of extracellular cargo and a method for its study in living cells.

Introduction

Cells require the intracellular degradation of extracellular cargo to utilize nutrients and down-regulate receptors.[1] LDL is perhaps the best-studied example of extracellular cargo.[1–3] The individual LDL particle is 22 nm in diameter and consists of apolipoprotein B-100 complexed in a roughly spherical particle of cholesteryl esters, phospholipids, and cholesterols.[1,4–6] Intracellular hydrolysis of LDL provides the necessary cholesterol for the formation of new membranes. Extensive studies of LDL have made it a benchmark for endocytic transport.[7–10] In brief, LDL binds to the LDL receptor, is internalized through a clathrin-mediated pathway, and is then transported to early endosomes. A decrease in the pH of the early endosomes causes LDL to dissociate from the receptor. The receptor is recycled to the cell surface while LDL proceeds through the endosomal pathway with the maturation of early endosomes to form late endosomes.[7,9]

LDL cannot be utilized by the cell without enzyme-mediated degradation. The intracellular degradation of extracellular cargo encompasses multiple chemical reactions mediated by lysosomal enzymes. To fully understand the degradative process it is necessary to observe the degradative event and associated transport as it occurs within a living cell. A key step in this process is the interaction of lysosomal enzymes with the endocytosed LDL. In a classic model of lysosomal degradation, a LDL-containing late endosome transports LDL to an enzyme-containing lysosome. Lysosomal enzymes degrade LDL and the degraded components are able to diffuse out of the lysosome for processing by the cell. A more detailed examination of the degradation pathway demonstrates that lysosomal enzymes are not restricted to the lysosomes, but are also present and active in early and late endosomes,[11–15] presenting a more complex picture of lysosomal degradation. Multiple types of extracellular cargo, including EGF and BSA, have been shown to undergo at least partial degradation before reaching the lysosomes.[11,13,16] LDL

School of Chemistry and Biochemistry and Petit Institute for Bioengineering and Bioscience, Georgia Institute of Technology, 901 Atlantic Drive, Atlanta, Georgia 30332, USA.
E-mail: christine.payne@chemistry.gatech.edu; Fax: 404-385-6057; Tel: 404-385-3125

† Electronic supplementary information (ESI) available: Figures S1–S4. See DOI: 10.1039/c0ib00035c

Insight, innovation, integration

To determine the cellular mechanism of low-density lipoprotein (LDL) degradation, we use single-particle tracking fluorescence microscopy to measure the interactions of LDL with GFP-labeled vesicles in live cells. Unique to our approach is the fluorescent labeling of LDL such that degradation corresponds to an increase in fluorescence intensity. In comparison to other approaches this method is dynamic, observing transient interactions; quantitative, measuring the time from entry of LDL into a vesicle to the degradation of the LDL particle; and specific, using GFP-proteins to fluorescently label populations of endocytic vesicles. This imaging approach provides direct evidence that LDL is degraded in the late endosome, upstream of the conventional picture of lysosomal degradation, with the lysosome serving to initiate degradation.

exposed to isolated and ruptured early and late endosomes is degraded, although prelysosomal degradation of LDL was not observed *in vivo*.[14]

The goal of our research is to measure the degradation of LDL directly, without the need to isolate endosomes or cargo. By imaging specific populations of vesicles and the degradative event simultaneously, we are able to not only determine which endosomal or lysosomal vesicle is responsible for degradation, but what specific interactions lead to degradation. These questions must be probed on an organelle-specific level, to distinguish late endosomes and lysosomes, and with sufficient time resolution to monitor the continual transport of LDL and endocytic vesicles within the cell. Fluorescence microscopy, combined with single particle tracking analysis, provides a method to follow the motion of individual vesicles and LDL particles within living cells.[17–19] Used in a two-color configuration, single particle tracking allows us to capture transient interactions that would not be detected in fixed cells. Organelle-specificity can be accomplished using GFP variants to label specific populations of endocytic vesicles, such as early and late endosomes.

Unique to our experiments is the ability to correlate interactions of vesicles with the enzyme-mediated degradation of LDL, all within live cells. This is accomplished with the use of a labeling scheme that takes advantage of the photophysical properties of a lipophilic fluorophore. By labeling the LDL particle with multiple fluorophores, the fluorescent signal from the LDL particle is quenched resulting in weak emission from the LDL particle. As the LDL particle degrades and the fluorophores are no longer in close proximity, the fluorescence intensity increases. Dequenching has been used previously to monitor changes in particle integrity, perhaps most commonly in virology.[20] We apply the same photophysical principles to monitor an intracellular enzymatic degradation. Our labeling scheme provides an extra dimension to fluorescence imaging. In addition to identifying interactions between endocytic vesicles and LDL, we simultaneously measure reactivity as an increase in intensity of the LDL particle is indicative of hydrolytic degradation. Using this labeling scheme it is possible to associate vesicle interactions with productive degradation.

Using this approach, we show that the degradation of LDL occurs in an endosome that is positive for the standard late endosomal protein Rab7. Transport to the late endosome is essential for degradation with minimal degradation observed in early endosomes or in wortmannin-treated cells. We measure the time from colocalization to degradation and find that it is highly correlated with the lysosomal protein, LAMP1, supporting a model in which lysosomes act as enzyme storage vesicles.[21–23] In the case of LDL, observing degradation as it occurs in living cells makes it possible to describe the complete endocytic pathway of LDL from internalization to degradation. More generally, characterizing the intracellular degradation of LDL provides a model for the intracellular degradation of extracellular cargo.

Results

Fluorescent labeling of LDL to observe intracellular degradation

LDL particles were labeled with multiple copies of the lipophilic dye, DiD. The standard labeling scheme for the LDL used in the experiments described below was ~200 DiD molecules for each LDL particle. As the LDL-DiD particle undergoes enzyme-mediated degradation and the DiD molecules are no longer in close proximity, we expect to observe a concomitant increase in fluorescence, described as dequenching.

Dequenching of LDL-DiD requires enzymatic activity

Characterization of the fluorescently labeled LDL, referred to as LDL-DiD, was first carried out *in vitro*, in the absence of cells, using a fluorimeter to measure changes in fluorescence emission (Fig. 1). Dequenching was measured as a ratio of fluorescence emission before and after incubation with trypsin (2 h, 37 °C), a degradative enzyme, or, as a control, at room temperature in the absence of enzyme. Incubation with trypsin at 37 °C resulted in a factor of 2.1 increase in fluorescence. No change in signal would be a value of 1. In comparison, identically labeled LDL-DiD incubated at room temperature or 37 °C for 2 h in the absence of trypsin showed a minimal increase in fluorescence intensity. Similarly, incubation at 37 °C or at pH 5.5, the pH of the late endosome,[1] resulted

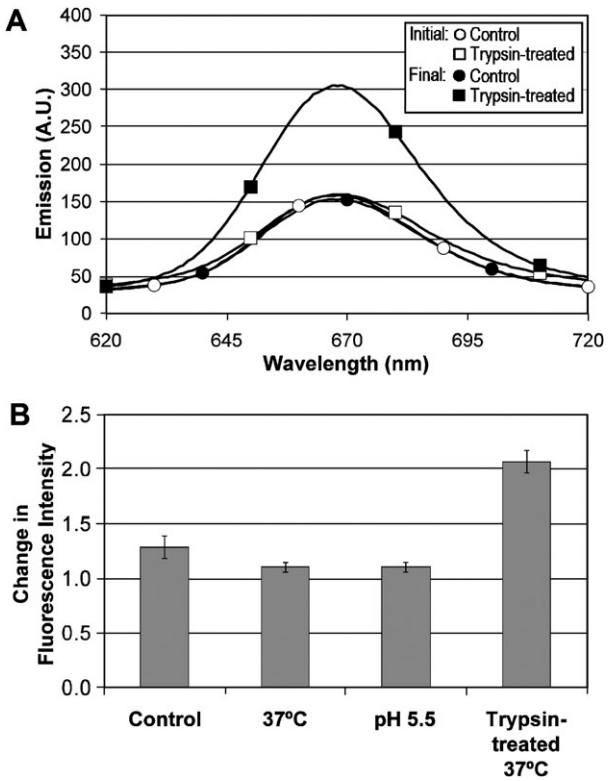

Fig. 1 ***In vitro*** **dequenching of LDL.** (A) Emission spectra of LDL-DiD in solution following excitation at 600 nm. Final spectra were measured after a 2 h incubation at either room temperature (control) or in the presence of trypsin at 37 °C. Absorption spectra showed little change after incubation (ESI Fig. S1). (B) Trypsin-treated LDL-DiD particles increased emission by a factor of 2.1. In the absence of trypsin, LDL-DiD showed only a slight increase in emission. A value of 1.0 indicates no change. The pH 5.5 incubation mimics the pH of the late endosome. Error bars represent the standard deviation of 3 experiments using the same LDL stock solution.

in little change in intensity. Emission measurements were normalized by the absorption of LDL-DiD before and after incubation, although there was relatively little change in absorption (ESI Fig. S1†).

Trypsin degrades LDL-DiD

To confirm that the increased fluorescence of LDL-DiD was a result of LDL degradation, we used gel electrophoresis to measure the degradation of the LDL apolipoprotein B-100. LDL-DiD and unlabeled LDL were incubated in the presence of trypsin (2 h, 37 °C) and then loaded onto a polyacrylamide gel (4–20% gradient). Cathepsin B, a known protease for apolipoprotein B-100,[24] was used as a comparison to trypsin. As expected from the dequenching results, trypsin leads to the appearance of multiple protein fragments, indicative of degradation (Fig. 2). Incubation with cathepsin B also leads to degradation. LDL incubated for 2 h in the absence of trypsin or cathepsin B does not show degradation. Additionally, labeling with DiD does not inhibit or alter degradation as LDL and LDL-DiD show similar staining patterns under all conditions.

Endocytosis of LDL is not disrupted by DiD

The endocytic pathway of LDL is well-characterized; LDL binds to the LDL receptor on the cell surface, is internalized *via* clathrin-mediated endocytosis, and is transported by early endosomes which mature into late endosomes.[1–3] It is important to ensure that the high degree of DiD labeling does not affect endocytosis of LDL-DiD. Endocytosis was tested using sparsely labeled LDL-DiD, with ~50 DiD molecules per LDL particle, as a control. To ensure internalization and transport were not disrupted by DiD labeling, colocalization with LAMP1, indicative of delivery to a terminal vesicle, was measured with confocal microscopy at a series of time points following incubation with LDL-DiD (Fig. 3A and B). Over a time period of 1 h, both LDL labeling schemes resulted in the same level of transport to LAMP1-vesicles with close to 100% colocalization at 1 h (Fig. 3E). No difference in internalization or transport was observed as a function of the degree of labeling.

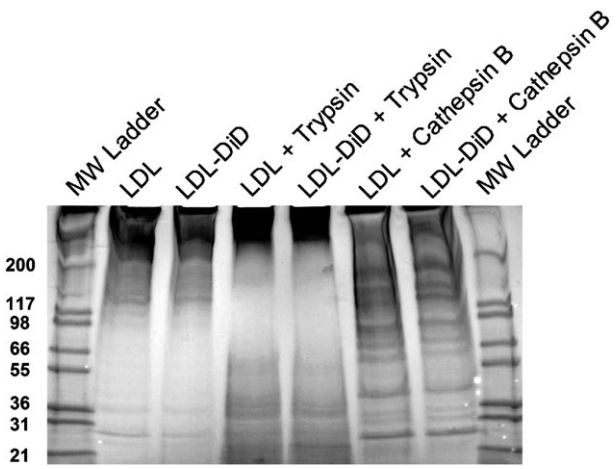

Fig. 2 Trypsin degrades LDL-DiD. Gel electrophoresis (4–20% gradient, polyacrylamide, SimplyBlue SafeStain) shows that treatment of LDL with trypsin or cathepsin B results in the appearance of multiple protein fragments in comparison to untreated LDL. DiD labeling of LDL (~200 DiD : LDL) does not inhibit degradation with trypsin or cathepsin B.

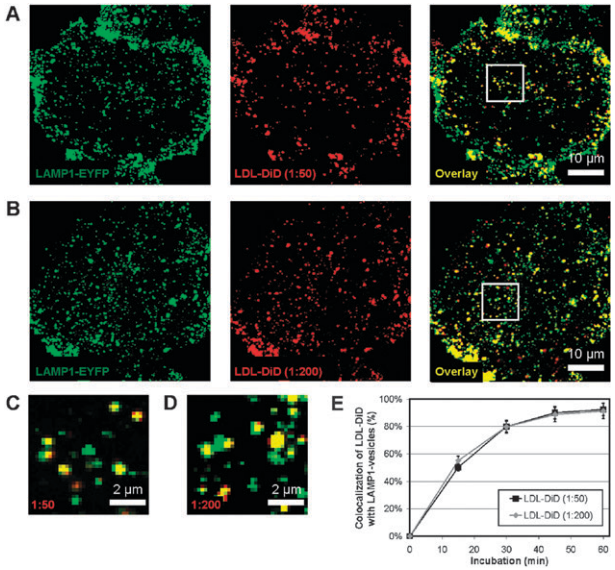

Fig. 3 Cellular internalization of LDL is not disrupted by DiD. (A) Confocal microscopy image of LDL labeled with 50 DiD molecules (red), a previously described labeling scheme,[10] and LAMP1-EYFP (green), following a 1 h incubation. LAMP1 serves as a marker of a terminal vesicle in the endocytic pathway. (B) Confocal microscopy image of LDL labeled with 200 DiD molecules (red) and LAMP1-EYFP (green) following a 1 h incubation. A ratio of 200 DiD : LDL was used in dequenching experiments. (C) Expanded region (shown in white box) of (A). (D) Expanded region (shown in white box) of (B). (E) Colocalization of LDL-DiD with LAMP1-EYFP, measured at increasing times following the addition of LDL-DiD, shows that the labeling density does not affect the intracellular transport of LDL-DiD. Colocalization was scored manually and error bars show the standard deviation for 40–240 LDL-DiD particles per cell in 3–5 cells.

Two-color single particle tracking of Rab7-endosomes and LDL-DiD

Single particle tracking allows us to follow the motion of fluorescently-labeled cargo or organelles, in real time, in live cells. In a two-color configuration, interactions between two spectrally-separable fluorophores can also be observed. This is especially important for transient interactions which cannot be detected in static fluorescence microscopy. Using the increase in LDL-DiD signal as a measure of degradation, two-color single particle tracking was used to correlate degradation of LDL with localization in a specific population of endosomes. Late endosomes were labeled with EYFP-Rab7 (Plasmid 20164, Addgene, Cambridge, MA).

Data are collected as movies from which the motion of Rab7-endosomes (green) and LDL-DiD (red) are tracked simultaneously (Fig. 4A). The intensity of the LDL-DiD particle is recorded during tracking measurements (Fig. 4B). LDL-DiD is considered dequenched if the intensity of the particle increases by a factor of 2 within a period of 100 s.

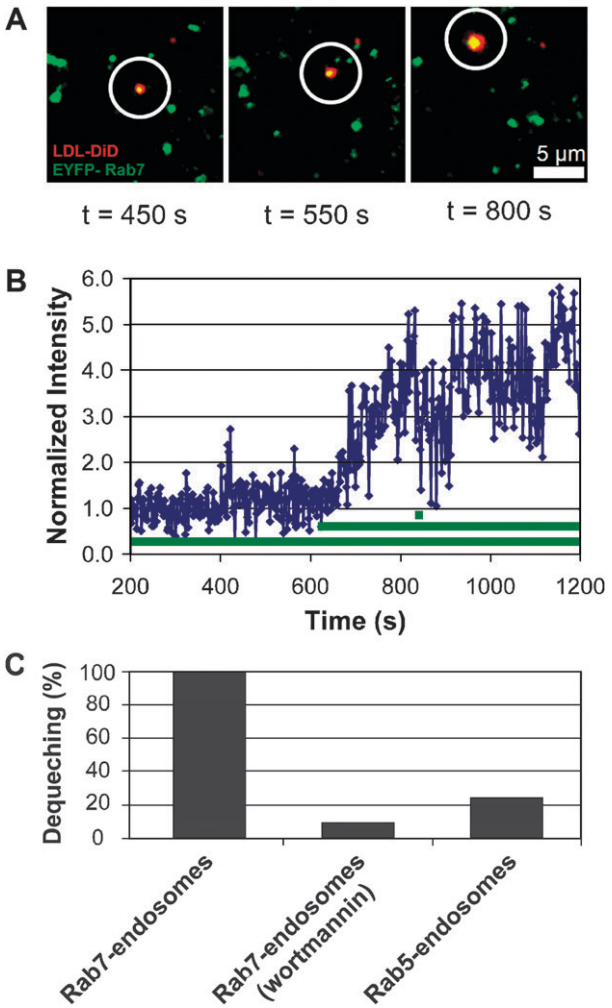

Fig. 4 Two-color single particle tracking of LDL-DiD and EYFP-Rab7. (A) Snapshots illustrating the dequenching of LDL-DiD (red) following interactions with an EYFP-Rab7 labeled endosome (green). Images are recorded at a rate of 0.5 Hz. (B) Intensity of the LDL-DiD particle as a function of time. The horizontal bars under the intensity trace indicate periods during which LDL-DiD was colocalized with a Rab7-endosome. (C) All dequenching events were observed during colocalization with a Rab7-endosome. The use of wortmannin to inhibit transport to the late endosomes significantly reduced the number of dequenching events observed. The observation of dequenching in ECFP-Rab5 labeled early endosomes was similarly rare. All dequenching percentages are normalized against untreated Rab7-endosomes.

The horizontal bars under the intensity trace indicate times during which the LDL-DiD particle was colocalized with a Rab7-endosome. To be considered colocalized, the respective fluorescent signals had to overlap and move through the cell together for a minimum of 4 s. The behavior displayed in this plot is representative of all the LDL-DiD particles that dequenched. Colocalization with Rab7-endosomes occurred soon after internalization of LDL-DiD, often before tracking began. Typically a second, or even third, Rab7-endosome fused with the initial Rab7-endosome containing the LDL-DiD particle. Dequenching occurred while the LDL-DiD particle was colocalized with Rab7-endosomes. Dequenching of LDL-DiD particles in Rab7-endosomes was observed for 19 LDL-DiD particles in 12 cells. Dequenching was not observed in the absence of colocalization with Rab7-endosomes.

Wortmannin treatment blocks the dequenching of LDL-DiD

To confirm that colocalization with Rab7-endosomes is necessary for dequenching, we used wortmannin, a PI(3)K inhibitor, to block endocytic transport of LDL to late endosomes.[25–29] The use of wortmannin (240 nM) to block transport to the Rab7-endosomes was measured with confocal microscopy following a 1 h incubation with LDL-DiD (ESI Fig. S2). A 60% decrease in colocalization with Rab7 was observed following wortmannin treatment, in good agreement with previous results.[10] In wortmannin-treated cells, with the transport to the late endosomes inhibited, dequenching of LDL-DiD was rarely observed (Fig. 4C). Only three, of twenty particles tracked in five cells, underwent dequenching in wortmannin-treated cells. These experiments also serve as a control to ensure that the increase in LDL fluorescence, interpreted as dequenching resulting from degradation, is not due to a decrease in the number of photoactive fluorophores following photobleaching or a change in microscope focus.

Colocalization with Rab5-endosomes does not lead to dequenching

As a second control, we tested whether entry into an early endosome could lead to dequenching, either due to lysosomal enzyme activity in the early endosomes[14] or as an artifact through the transfer of DiD to the endosomal membrane. While the wortmannin experiments address these questions by blocking transport of LDL-DiD to the late endosomes, we also tested this in a drug-free assay. We labeled the early endosomes with EGFP-Rab5, an early endosomal protein,[29,30] which was confirmed with EEA1 colocalization (data not shown).[29–31] Two-color imaging experiments showed very little dequenching during the interaction of LDL-DiD with Rab5-endosomes (Fig. 4C). Only five, of twenty-four particles tracked in seven cells, underwent dequenching in Rab5-endosomes, further demonstrating that the interaction with Rab7-endosomes is necessary and specific for dequenching.

Two-color single particle tracking of LAMP1-vesicles and LDL-DiD

The observed degradation of LDL-DiD in a Rab7-endosome raised the question of the role of the lysosome, the canonical degradative vesicle, in this process. Despite the name, lysosome-associated membrane protein 1 (LAMP1) is associated with late endosomes as well as lysosomes.[21,32] For this reason, we refer to the LAMP1-associated organelle generically as a vesicle. In the BS-C-1 cells used in these experiments, we measure $>80\%$ colocalization of ECFP-Rab7 and LAMP1-EYFP in 12 cells (Fig. 5A). Two-color live cell imaging demonstrated that these two populations of vesicles, while highly colocalized, are distinct and dynamic (Fig. 5B). Tracking these vesicles over time showed that Rab7 and LAMP1 are typically colocalized, but undergo short periods of separation before pairing with new vesicles (Fig. 5C). A histogram of times during which Rab7 and LAMP1 are

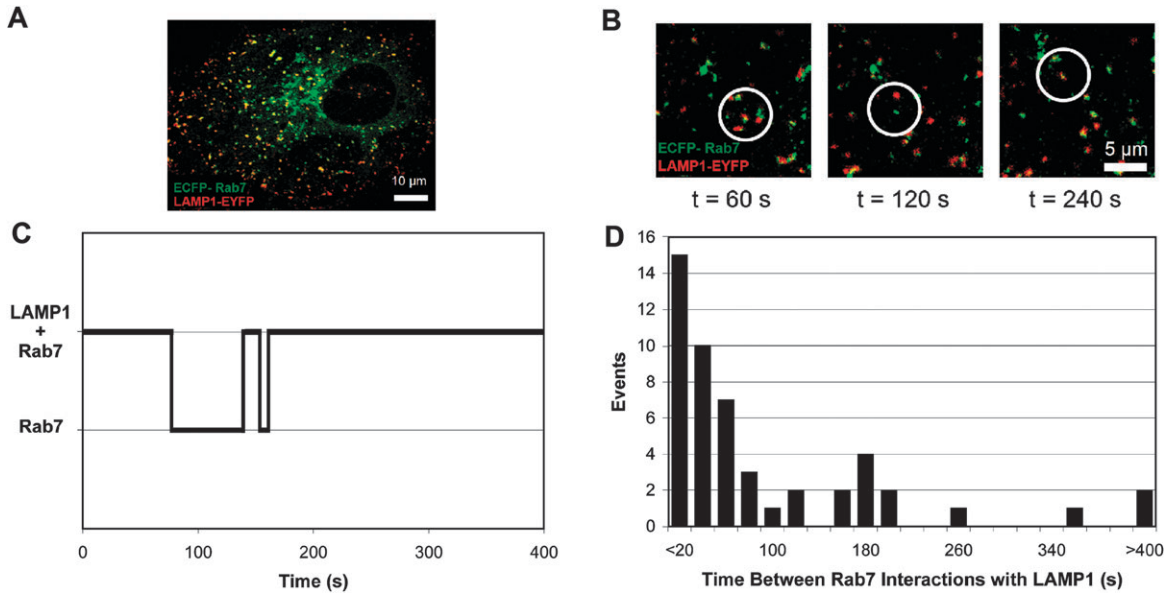

Fig. 5 Interaction of Rab7-endosomes and LAMP1-vesicles. (A) Colocalization of ECFP-Rab7 (green) and LAMP1-EYFP (red). (B) Snapshots illustrating two-color single particle tracking of ECFP-Rab7 (green) and LAMP1-EYFP (red) show a Rab7- and LAMP1-positive vesicle that separates before the Rab7-endosome interacts with a different LAMP1-vesicle. (C) Measurement of colocalization as a function of time. (D) A histogram of time periods during with Rab7 and LAMP1 are not colocalized. The maximum period of observation was 1200 s.

separated showed that most periods of separation are <100 s (Fig. 5D). On average, 10% of Rab7-endosomes and LAMP1-vesicles are found in the cell as distinct, non-colocalized, vesicles.

The short periods during which LAMP1-vesicles were not associated with Rab7-endosomes encouraged us to examine the role of LAMP1-vesicles in LDL degradation. Using the same two-color tracking scheme as described for EYFP-Rab7 and LDL-DiD, LAMP1-EYFP and LDL-DiD were imaged simultaneously (Fig. 6A). Analysis focused on LDL-DiD particles that were initially not colocalized with LAMP1-EYFP. We observed that the colocalization of LAMP1-vesicles with these LDL-DiD particles led to an increase in fluorescence for 28% of the 78 interactions tracked in 12 cells. Intensity traces were then analyzed for the 22 dequenching events (Fig. 6B). Dequenching events following the interaction of LDL-DiD with LAMP1-vesicles differed from the dequenching events observed following Rab7-endosome colocalization. While Rab7-endosomes and LDL had long periods of colocalization before dequenching, LAMP1 colocalization was followed immediately by dequenching. Following dequenching of LDL-DiD, a separation of LAMP1 from the LDL particle was occasionally observed although this aspect of vesicle interactions was not probed in the course of these experiments.

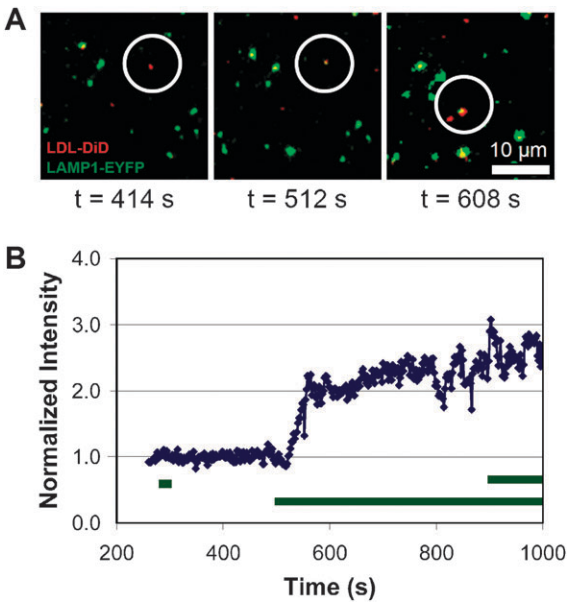

Fig. 6 Two-color single particle tracking of LDL-DiD and LAMP1-EYFP. (A) Snapshots illustrating the dequenching of LDL-DiD (red) following interactions with a LAMP1-EYFP labeled vesicle (green). Images are recorded at a rate of 0.5 Hz. (B) Intensity of the LDL-DiD particle as a function of time. The horizontal bars under the intensity trace indicate periods during which LDL-DiD was colocalized with a LAMP1-vesicle.

Time from colocalization to dequenching

For both the Rab7 and LAMP1 data, the time from colocalization to dequenching can be measured to test for possible correlations. The time from the colocalization of LDL-DiD with a Rab7-endosome to the dequenching of LDL-DiD varies, but occurs after at least 180 s for $>50\%$ of dequenching events. (Fig. 7A). This is a conservative measure as many LDL-DiD particles are already localized in Rab7-endosomes at the start of imaging. In comparison, colocalization with LAMP1-vesicles is followed shortly by dequenching (Fig. 7B). The majority of dequenching events occur within 30 s of colocalization with a LAMP1-vesicle.

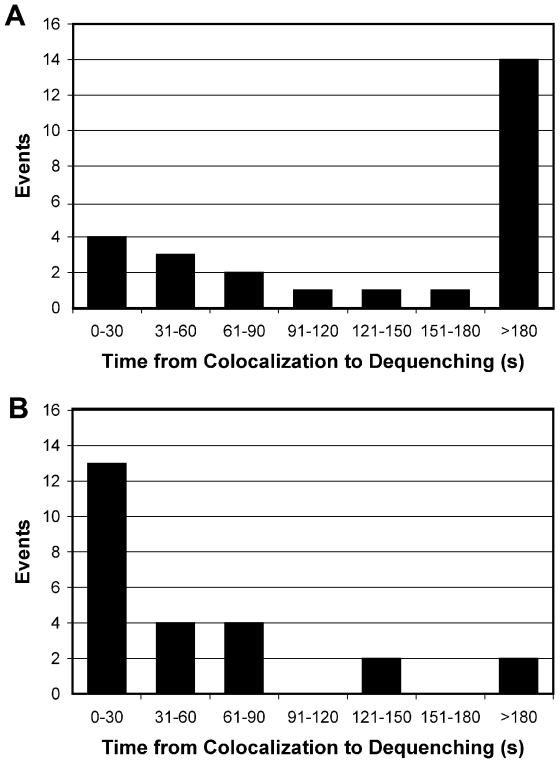

Fig. 7 Time from interaction of Rab7-endosomes and LAMP1-vesicles with LDL-DiD to dequenching of LDL-DiD. (A) Rab7-endosomes. A histogram of times measured from colocalization with Rab7-endosomes to LDL-DiD dequenching shows that dequenching typically occurs after long (>180 s) periods of colocalization. (B) LAMP1-vesicles. A histogram of times measured from colocalization with LAMP1-vesicles to LDL-DiD dequenching shows that dequenching typically occurs within 30 s of colocalization.

Discussion

The goal of this research is to use a quantitative approach to relate endosomal and lysosomal dynamics to the degradation of endocytic cargo. We chose LDL, a classic endocytic marker, as the extracellular cargo to probe for degradation. While the endocytic pathway of LDL is well-studied, the final degradative step had not previously been characterized in live cells. Using a highly labeled LDL particle, we were able to correlate an increase in fluorescence intensity with the degradation of the LDL particle. Using two-color fluorescence microscopy, we measured colocalization of LDL-DiD with Rab7-endosomes and LAMP1-vesicles while simultaneously measuring the degradation of LDL. Our approach is dynamic, observing transient interactions in live cells; quantitative, measuring the time from colocalization to degradation; and specific, using GFP-protein markers of endosome populations.

This research provides the first direct observation, in intact live cells, of enzyme-mediated degradation occurring in the late endosome (Fig. 4). These observations build on previous *in vitro* assays which showed that lysosomal enzymes are both present and active in the early and late endosomes and that degradation of EGF, BSA, and LDL could occur before entry into a lysosome,[11–14,16] in contrast with the classic model of lysosomal degradation. Most similarly, previous work has described the degradation of LDL after exposure to isolated and ruptured early and late endosomes.[14] Despite the observation of degradation *in vitro*, LDL degradation was not observed *in vivo*. To some extent, single cell imaging experiments provide a link between *in vitro* experiments with isolated endosomes and *in vivo* experiments measuring LDL degradation in rat livers. *In vitro*, degradation was observed following incubation with isolated and ruptured early and late endosomes held at a pH of 4.3 to 5. In comparison, we do not observe degradation within the early endosomes. With intact cells, it is likely that the pH of the early endosomes is higher than 5, thereby inhibiting enzyme activity.[1] It is more difficult to make comparisons to *in vivo* experiments, although it is possible that the short incubations times (7.5 min and 15 min) used for *in vivo* experiments were insufficient for internalization and transport following intravenous injection of radio-labeled LDL.

While Rab7 is a well-established marker for late endosomes,[7,32–36] the description of LAMP1-vesicles is more difficult. LAMP1 associates with both late endosomes and lysosomes.[21,32] The BS-C-1 cells used in these experiments show a high degree of colocalization between Rab7 and LAMP1 (Fig. 5A) with degradation occurring within vesicles that are positive for both proteins. These observations raise the broader question of the differences between late endosomes and lysosomes. MPR is the distinguishing feature of late endosomes, with lysosomes defined as MPR-negative.[21,32] Previous work has described a distinct set of vesicles, resulting from the fusion of late endosomes and lysosomes, that have been isolated and identified as hybrid organelles.[37,38] These vesicles are MPR positive and contain lysosomal enzymes. Our results are consistent with the existence of this form of hybrid organelle which has late endosomal character, shown by the presence of Rab7, with sufficient enzyme activity for the degradation of LDL. Most similar to our work are previous results demonstrating degradation of an isotopically labeled ovalbumin complex in Rab7-endosomes.[23] Using subcellular fractionation it was found that degradation of the ovalbumin complex occurred in Rab7-endosomes rather than lysosomes, which were defined as a lysosomal enzyme-rich population of vesicles. While late endosomes contained only 20% of lysosomal enzyme activity, they were responsible for the degradation of 80% of the endocytic cargo.

More subtle mechanistic details provided by single particle tracking highlight the differences between Rab7-endosomes and LAMP1-vesicles in the degradation of LDL. Despite the high level of colocalization between Rab7 and LAMP1, two-color single particle tracking measurements show that these proteins are associated with distinct, highly dynamic vesicles. Most interesting are the differences observed between Rab7 and LAMP1 in the degradation of LDL. Entry of LDL into a LAMP1-vesicle leads to the rapid degradation of the LDL particle. In comparison, no correlation is observed between entry into a Rab7-endosome and degradation of LDL. This behavior suggests that LAMP1 defines a more reactive, enzyme rich, vesicle that triggers the degradation of LDL. Taken together, these results support a previously proposed model in which lysosomes function as enzyme storage vesicles that deliver enzymes to late endosomes or hybrid organelles for degradation.[21–23]

Experimental

Cell culture

BS-C-1 cells (ATCC, Manassas, VA) were maintained in a 37 °C, 5% carbon dioxide environment in Minimum Essential Medium (MEM, Invitrogen, Carlsbad, CA) with 10% (v/v) fetal bovine serum (FBS, Invitrogen). Cells were passaged every 4 days. For fluorescence imaging, cells were cultured in 35 mm glass-bottom cell culture dishes (MatTek, Ashland, MA).

Expression of fluorescently-labeled endocytic proteins

Rab7-endosomes were labeled with EYFP-Rab7 (Plasmid 20164, Addgene, Cambridge, MA)[7] in transiently transfected cells or stably with ECFP-Rab7 (a gift from S. Pfeffer). In the BS-C-1 cells used in these experiments, Rab7 shows close to 70% colocalization with the cation-independent mannose-6-phosphate receptor (MPR; ESI Fig. S3). Rab5-endosomes were labeled with EGFP-Rab5 (a gift from M. Zerial) in transiently transfected cells and confirmed with EEA1 colocalization (data not shown).[29–31] LAMP1-vesicles were fluorescently labeled with LAMP1-EYFP (Plasmid 1816, Addgene, Cambridge, MA) in a stably transfected cell line.[39] Immunofluorescence with LAMP2 was used to confirm expression (ESI Fig. S4). Transfections were performed using the FuGENE 6 (Roche, Indianapolis, IN) transfection reagent 24 h after plating. Experiments were carried out 24 h after transfection.

Fluorescent labeling, *in vitro* degradation, and endocytosis of LDL

Human LDL (BT-903, Biomedical Technologies, Stoughton, MA) was labeled with 1,1′-dioctadecyl-3,3,3′,3′-tetramethylindodicarbocyanine perchlorate (DiD, D-307, Invitrogen) at a concentration of 1.8 mM for a ratio of 200 DiD : LDL. LDL and DiD were mixed every 10 min for 1 h before removal of excess dye on a NAP5 size exclusion column (17–0853-02, GE Healthcare, Buckinghamshire, UK). The ratio of DiD molecules per LDL particle was measured using a UV-Vis spectrophotometer (DU800, Beckman Coulter, Fullerton, CA). A spectrofluorophotometer (RF-5301PC, Shimadzu, Japan) was used to measure changes in fluorescence emission. LDL-DiD was excited at 600 nm.

To verify that DiD did not affect LDL degradation, LDL-DiD and unlabeled LDL (both 40 μg) were incubated with either cathepsin B (1 μg in 0.1 M sodium acetate at pH 5.5; SE-198, Enzo, Plymouth Meeting, PA) or trypsin-EDTA (0.25 mg mL^{-1}, 25200-072, Invitrogen), which we refer to as trypsin in the text. The reaction products were analyzed with gel electrophoresis (Fig. 2). Initial mixtures were prepared on ice before incubation at 37 °C for 2 h. The reaction product (12 μg) was loaded onto a precast polyacrylamide gel (4–20%, 161–1105, Bio-Rad, Hercules, CA) and run at 140 V for 1 h. Gels were stained with SimplyBlue SafeStain (LC6060, Invitrogen) for 1 h and destained in water for at least 2 h.

For cellular imaging experiments, cells were incubated with 10 μg mL^{-1} of LDL-DiD for 10 min at 37 °C. Immediately before imaging experiments cells were washed with phenol-red free MEM (Invitrogen) buffered with 0.1 M HEPES. For single particle tracking experiments the imaging medium was supplemented with 2% FBS, 1% glucose, and an oxygen scavenger (0.4 mg mL^{-1} glucose oxidase and 2 μL mL^{-1} catalase) was added to the cell culture medium.

Wortmannin treatment

Wortmannin (W1628, Sigma, St Louis, MO) was used to inhibit phosphatidylinositol-3-OH kinase (PI(3)K),[25,26,40] thereby disrupting transport of LDL-DiD to the late endosomes.[28,29] Cells were incubated in full growth medium supplemented with 240 nM wortmannin for 30 min prior to addition of LDL-DiD. Wortmannin remained present for the duration of the experiment. The efficiency of the wortmannin treatment was examined by colocalization of LDL-DiD with EYFP-Rab7 (ESI Fig. S2).

Immunofluorescence

For the majority of experiments, cells were fixed with 2% formaldehyde for 40 min at room temperature and permeabilized (3% BSA, 10% FBS, 0.5% Triton-X 100 in PBS) for 15 min at room temperature. Cells were incubated for 1 h in blocking buffer (10% FBS, 3% BSA in PBS) before the addition of each antibody. The primary antibody was added to cells at 1–5 : 1000 dilutions in blocking buffer and incubated for 3–18 h at 4 °C. The secondary antibody was added to cells at a 1 : 1000 dilution in blocking buffer and incubated for 30 min at room temperature. Cells were washed (0.3% BSA, 0.1% Triton-X 100 in PBS) three times between each step. The exception to this was immunofluorescence against the cation-independent MPR. Based on the method of J.X. Kang, *et al.*,[41] cells were fixed with 4% formaldehyde for 30 min at room temperature and permeabilized (0.1% Triton-X 100 in PBS) for 5 min at room temperature. The primary antibody was added to cells at a 1 : 400 dilution in blocking buffer (10% FBS, 3% BSA in PBS) and incubated for 1 h at room temperature. The secondary antibody was added to cells at a 1 : 1000 dilution in blocking buffer and incubated for 30 min at room temperature. Cells were incubated in blocking buffer for 1 h prior to the addition of each antibody and washed in PBS three times between each step. Three primary antibodies were used in the course of these experiments: mouse MPR (MA1-066, Fisher Scientific), mouse LAMP2 (ab25631, Abcam, Cambridge, MA), and mouse EEA1 (ab15846, Abcam). One secondary antibody was used for all experiments: Cy5 rabbit anti-mouse (AP160S, Chemicon, Temecula, CA).

Single particle tracking fluorescence microscopy

For two-color, single particle tracking experiments, an inverted microscope (Olympus IX71, Center Valley, PA) in an *epi*-fluorescent configuration with a 1.45 N A, 60x, oil immersion objective (Olympus) was used. Excitation was supplied by three lasers: a tunable argon ion laser (35-LAP-431-208, Melles Griot, Carlsbad, CA), a green diode (Green532, CrystaLaser, Reno, NV), and a red diode (635-25C, Coherent, Santa Clara, CA). Excitation beams were overlapped using dichroic mirrors (Z488RSC and Z532BCM, Chroma, Rockingham, VT) and focused on the back focal plane of the microscope objective. A shutter (Uniblitz, Rochester, NY) limited exposure of the cells to the lasers. Cells were

illuminated by multiple laser lines using the appropriate dichroic mirror (Z458/532/633RPC, Z488/532/633RPC, Z514/633RPC, Chroma). Emission was separated into two channels based on wavelength using a 620 nm long pass filter (620DCXR, Chroma). Excitation light was filtered out of the emission by the appropriate filters: ECFP—Brightline 483/32 (Semrock, Rochester, NY), EGFP—HQ550/50 (Chroma), EYFP—HQ580/50 (Chroma), DiD—HQ680/60 (Chroma). A second 620 nm long pass filter (Chroma) was used to image both emission paths side by side on a single CDD camera (DU-888, Andor, South Windsor, CT). Images were recorded at a rate of 0.5 frames/s with a 200 ms exposure. Experiments were conducted at 37 °C.

Confocal microscopy

Confocal microscopy was carried out with a LSM 510 confocal microscope (Carl Zeiss Inc., Jena, Germany) using a 1.40 N.A., 63×, oil immersion objective. EYFP and EGFP were excited with the 488 nm line of an argon ion laser. For EYFP, a 530-600 nm band pass filter was used and for EGFP a 505-530 nm band pass filter was used. LDL-DiD was excited with the 633 nm line of a helium-neon laser and emission was filtered through a 650 nm long pass filter. The pinhole was set to obtain a 1 μm thick optical slice.

Data analysis

Image J (http://rsb.info.nih.gov/ij/) was used for tracking and quantifying colocalization. Particle tracking was performed with the Image J plugin, "Manual Tracking" (http://rsb.info.nih.gov/ij/plugins/track/track.html) and colocalization was assisted by "Image5D" (http://rsb.info.nih.gov/ij/plugins/image5d.html). Images for publication were background subtracted and intensities were adjusted equally within each data set.

Conclusions

To understand the final step in the endocytic pathway of LDL, we observed the degradation of LDL, and associated transport, as it occurred inside a living cell. To detect degradation, we used an LDL particle heavily labeled with the fluorophore DiD. Control experiments were carried out to demonstrate that degradation of the LDL particle corresponded to an increase in fluorescence. Late endosomes were specifically labeled with EYFP-Rab7 to directly monitor the interaction of these vesicles with the LDL cargo. Using two-color fluorescence microscopy, we measured the transient colocalization of LDL-DiD with fluorescently-labeled late endosomes while simultaneously measuring the degradation of LDL. This imaging approach provides direct evidence that the degradation of LDL occurs in the late endosome. Minimal degradation was observed in the early endosomes. Measuring the time to degradation following interaction with vesicles suggests that LAMP1-vesicles may serve as enzyme storage vesicles that deliver enzymes to late endosomes, forming a hybrid organelle, in which degradation occurs. In the case of LDL, understanding the degradation of LDL completes the description of this important endocytic pathway. More generally, characterizing the intracellular degradation of LDL provides a model for endosomal-lysosomal degradation. The use of single particle tracking fluorescence microscopy combined with dequenching demonstrates a new method to address questions of cellular transport and protein degradation in intact cells.

Acknowledgements

We thank M. Zerial and S. Pfeffer for their generous gifts of the EGFP-Rab5 and ECFP-Rab7 plasmids, respectively; Dr Mary Peek for her support of portions of this research as a Biochemistry II project; Paul Park for his *in vitro* measurements; and Jenna Tomlinson (NSF-REU, 2008) for her assistance with stably transfected cell lines. This work is supported in part by the National Institutes of Health (NIAID) through a Research Scholar Development Award (K22AI068673) to CKP. NCF was partially supported through a President's Undergraduate Research Award (Georgia Tech).

References

1 B. Alberts, D. Bray, J. Lewis, M. Raff, K. Roberts and J. D. Watson, *Molecular Biology of the Cell*, Garland Publishing, New York, 1994.
2 J. L. Goldstein, M. S. Brown, R. G. W. Anderson, D. W. Russell and W. J. Schneider, *Annu. Rev. Cell Biol.*, 1985, **1**, 1–39.
3 C. G. Davis, J. L. Goldstein, T. C. Sudhof, R. G. W. Anderson, D. W. Russell and M. S. Brown, *Nature*, 1987, **326**, 760–765.
4 D. Voet and J. G. Voet, *Biochemistry*, John Wiley & Sons, New Jersey, 2004.
5 J. P. Segrest, M. K. Jones, H. De Loof and N. Dashti, *J. Lipid Res.*, 2001, **42**, 1346–1367.
6 T. Hevonoja, M. O. Pentikainen, M. T. Hyvonen, P. T. Kovanen and M. Ala-Korpela, *Biochim. Biophys. Acta, Mol. Cell Biol. Lipids*, 2000, **1488**, 189–210.
7 M. Lakadamyali, M. J. Rust and X. Zhuang, *Cell*, 2006, **124**, 997–1009.
8 K. W. Dunn, T. E. McGraw and F. R. Maxfield, *J. Cell Biol.*, 1989, **109**, 3303–3314.
9 J. Rink, E. Ghigo, Y. Kalaidzidis and M. Zerial, *Cell*, 2005, **122**, 735–749.
10 C. K. Payne, S. A. Jones, C. Chen and X. W. Zhuang, *Traffic*, 2007, **8**, 389–401.
11 F. Authier, B. I. Posner and J. J. M. Bergeron, *FEBS Lett.*, 1996, **389**, 55–60.
12 R. Bowser and R. F. Murphy, *J. Cell. Physiol.*, 1990, **143**, 110–117.
13 C. A. Renfrew and A. L. Hubbard, *J. Biol. Chem.*, 1991, **266**, 4348–4356.
14 E. A. Runquist and R. J. Havel, *J. Biol. Chem.*, 1991, **266**, 22557–22563.
15 M. Roederer, R. Bowser and R. F. Murphy, *J. Cell. Physiol.*, 1987, **131**, 200–209.
16 S. Diment and P. Stahl, *J. Biol. Chem.*, 1985, **260**, 5311–5317.
17 B. Brandenburg and X. W. Zhuang, *Nat. Rev. Microbiol.*, 2007, **5**, 197–208.
18 E. M. Damm and L. Pelkmans, *Cell. Microbiol.*, 2006, **8**, 1219–1227.
19 C. K. Payne, *Nanomedicine*, 2007, **2**, 847–860.
20 A. Loyter, V. Citovsky and R. Blumenthal, *Methods Biochem. Anal.*, 1988, **33**, 129–164.
21 C. S. Pillay, E. Elliott and C. Dennison, *Biochem. J.*, 2002, **363**, 417–429.
22 J. P. Luzio, P. R. Pryor and N. A. Bright, *Nat. Rev. Mol. Cell Biol.*, 2007, **8**, 622–632.
23 T. E. Tjelle, A. Brech, L. K. Juvet, G. Griffiths and T. Berg, *J. Cell Sci.*, 1996, **109**, 2905–2914.
24 M. Linke, R. E. Gordon, M. Brillard, F. Lecaille, G. Lalmanach and D. Bromme, *Biol. Chem.*, 2006, **387**, 1295–1303.
25 G. Li, C. D'Souza-Schorey, M. A. Barbieri, R. L. Roberts, A. Klippel, L. T. Williams and P. D. Stahl, *Proc. Natl. Acad. Sci. U. S. A.*, 1995, **92**, 10207–10211.

26 J. L. Martys, C. Wjasow, D. M. Gangi, M. C. Kielian, T. E. McGraw and J. M. Backer, *J. Biol. Chem*., 1996, **271**, 10953–10962.
27 A. Petiot, J. Faure, H. Stenmark and J. Gruenberg, *J. Cell Biol*., 2003, **162**, 971–979.
28 J. Gruenberg and H. Stenmark, *Nat. Rev. Mol. Cell Biol*., 2004, **5**, 317–323.
29 A. Simonsen, R. Lippe, S. Christoforidis, J. M. Gaullier, A. Brech, J. Callaghan, B. H. Toh, C. Murphy, M. Zerial and H. Stenmark, *Nature*, 1998, **394**, 494–498.
30 P. Chavrier, R. G. Parton, H. P. Hauri, K. Simons and M. Zerial, *Cell*, 1990, **62**, 317–329.
31 S. Christoforidis, H. M. McBride, R. D. Burgoyne and M. Zerial, *Nature*, 1999, **397**, 621–625.
32 M. J. Clague, *Biochem. J*., 1998, **336**, 271–282.
33 Y. Feng, B. Press and A. Wandinger-Ness, *J. Cell Biol*., 1995, **131**, 1435–1452.
34 T. Soldati, C. Rancano, H. Geissler and S. R. Pfeffer, *J. Biol. Chem*., 1995, **270**, 25541–25548.
35 R. Vitelli, M. Santillo, D. Lattero, M. Chiariello, M. Bifulco, C. B. Bruni and C. Bucci, *J. Biol. Chem*., 1997, **272**, 4391–4397.
36 P. Barbero, L. Bittova and S. R. Pfeffer, *J. Cell Biol*., 2002, **156**, 511–518.
37 B. M. Mullock, N. A. Bright, G. W. Fearon, S. R. Gray and J. P. Luzio, *J. Cell Biol*., 1998, **140**, 591–601.
38 N. A. Bright, B. J. Reaves, B. M. Mullock and J. P. Luzio, *J. Cell Sci*., 1997, **110**, 2027–2040.
39 N. M. Sherer, M. J. Lehmann, L. F. Jimenez-Soto, A. Ingmundson, S. M. Horner, G. Cicchetti, P. G. Allen, M. Pypaert, J. M. Cunningham and W. Mothes, *Traffic*, 2003, **4**, 785–801.
40 H. Shpetner, M. Joly, D. Hartley and S. Corvera, *J. Cell Biol*., 1996, **132**, 595–605.
41 J. X. Kang, J. Bell, A. Leaf, R. L. Beard and R. A. S. Chandraratna, *Proc. Natl. Acad. Sci. U. S. A*., 1998, **95**, 13687–13691.

